Effect of inorganic salt ions on the adsorption of quinoline using coal powder

Yue Bian, Hao Sun, Yunxiao Luo, Qieyuan Gao, Guosheng Li and Yongtian Wang

ABSTRACT

In this study, coal powder was used as the adsorbent for quinoline. The effect of inorganic salt ions on the adsorption was explored, and the results suggest that the addition of inorganic salt ions can enhance both the removal rate and the amount of quinoline adsorbed. The removal rate and adsorbed amount of quinoline were 83.87% and 1.26 mg/g without inorganic salt ions. Under the same adsorption conditions, the removal rate and adsorbed amount of quinoline could reach 90.21% and 1.35 mg/g when Na^+ was present in the solution, and 94.47% and 1.42 mg/g with the presence of Ca^{2+}. In addition, the adsorption of quinoline using coal fitted the Freundlich isothermal adsorption model. Changes in the Gibbs free energy, entropy and heat of adsorption were all negative, indicating that the adsorption was spontaneous and exothermic. The changes in the absolute value of Gibbs free energy under both Na^+ and Ca^{2+} were higher than that in the blank (without inorganic salt ions). The pseudo-second-order kinetic model was found to fit the adsorption kinetic data well, and the activation energy of adsorption under Na^+ and Ca^{2+} were lower than that in the blank. These indicate that the addition of inorganic salt ions was beneficial to the adsorption process.

Key words | adsorption process, industrial wastewater treatment, kinetic models, Langmuir and Freundlich isotherms, nitrogenous organic compounds

Yue Bian
China Coal Research Institute Company of Energy Conservation,
China Coal Research Institute,
Beijing 100013,
China

Yue Bian
Hao Sun
Yunxiao Luo
Qieyuan Gao
Guosheng Li
School of Chemical Engineering and Technology,
China University of Mining and Technology,
Xuzhou 221116, Jiangsu,
China

Yongtian Wang (corresponding author)
Chinese National Engineering Research Center of
Coal Preparation and Purification,
Xuzhou 221116, Jiangsu,
China
E-mail: 13705219495@139.com

INTRODUCTION

Quinoline is a typical nitrogenous organic compound commonly seen in the petroleum, coal tar, coal gas and oil shale processing industries. It is widely used as a raw material and solvent in the dye, paint, fungicide and wood-processing industries (Padoley *et al.* 2008; Rameshraja & Srivastava 2012; Wang *et al.* 2016). However, quinoline is a risk to the environment and humans due to being highly toxic. It has a good solubility and low biodegradability which makes it penetrate easily into the soil and groundwater, causing environmental problems and illness.

Physico-chemical and biological methods have been used to treat wastewater containing quinoline. In addition, multiple adsorbents such as granular activated carbon and bagasse fly ash (Rameshraja & Srivastava 2012), kaolinite and montmorillonite (Chen 2002), mesoporous molecular sieve Ti-HMS (Thomas *et al.* 2010), Pt (Santarossa *et al.* 2008), fibrous silicates and Patagonian saponite (Vico &

Acebal 2006), combusted rundle spent shale (Zhu *et al.* 1995) have been used in the removal of quinoline. However, various problems including high cost, desorption difficulty after adsorption, transfer of organic pollutants after desorption, poor adsorption effect after multiple adsorption and desorption make it difficult for these adsorbents to be scaled up for industrial application. So an adsorbent with the lowest possible price that does not require regeneration is very desirable.

Coal is an important energy resource widely used with other fossil fuels such as oil and natural gas. It has relatively large pores and specific surface area, and has been tested to adsorb methane, carbon monoxide and other gases well at the laboratory scale (Hao *et al.* 2013; Jian *et al.* 2015). In addition, Wang *et al.* described a method of wastewater treatment using coal as a potential adsorption material and this technology has been successfully used in industrial

production (Wang *et al.* 2014). It should be noted that the requirement for a sustainable industrial wastewater treatment technology should include the following key elements: a sorbent with good sorption properties along with a low price that could go back into the coking system after adsorption instead of entering a regeneration process (Gao *et al.* 2016a, 2016b). The study found that the chemical oxygen demand (COD) was reduced from 178.99 mg/L to 43.56 mg/L, and the removal rate reached 75.66%, using coking coal powder to treat coking wastewater (Gao *et al.* 2015). It was interesting to find that the coking coal had a higher adsorption capacity in an acidic solution (Gao *et al.* 2016a, 2016b). This may be attributed to a greater specific surface area produced by minerals dissolving to form inorganic salt ions under the addition of acid, which enhanced the adsorption effect. In addition, the dissolved inorganic salt ions may have had an impact on the adsorption of pollutants using coking coal.

As can be seen, the use of coal as an adsorbent to treat industrial wastewater, especially the adsorption process under the influence of inorganic ions is still poorly understood. This paper explores the effect of inorganic salt ions on the adsorption of quinoline using coal powders, taking Na^+ and Ca^{2+} as examples. The data were fitted to Langmuir and Freundlich isothermal adsorption models, and various thermodynamic parameters were also calculated. Sorption kinetics was studied using pseudo-first-order and pseudo-second-order kinetic models. The ζ-potentials (zeta potentials) of coal particles in the solution with different inorganic salt ion concentrations were measured to explain the effect of the inorganic ions on adsorption.

MATERIALS AND METHODS

Materials

The low-rank coal was obtained from Shenmu, Shaanxi, China. It was crushed to 3 mm, and then ground so that 85% of the coal sample was below 200 mesh before using as the adsorbent for this work. The physical and chemical properties of the coal sample were analyzed using X-ray fluorescence (XRF, Model S8 TIGER, Bruker AXS GmbH, element detection range: Be (4) ~U (92)), X-ray diffraction (XRD, Model D8 Advance, Bruker AXS GmbH, X-ray tube voltage 40 kV, current 30 mA, anode target material Cu target, radiation Ka), scanning electron microscope (SEM, Model FEI Quanta TM 250, Thermo Fisher Scientific Inc., scanning acceleration voltage 30 kV, resolution less than

3 nm, coating treatment sprayed on before test) and BET automatic nitrogen adsorption instrument (BELSORP-max, BEL JAPAN Inc.).

A 1 g/L quinoline stock solution was prepared by dissolving 1 g quinoline in deionized water in a 1 L volumetric flask and stirring well to ensure the quinoline dissolved completely. The quinoline was supplied by Kemiou Chemical Reagent Co., Ltd. NaCl and $CaCl_2$, supplied by Sinopharm Chemical Reagent Co., Ltd, were added to prepare solutions of different inorganic salt ion concentrations, respectively. All chemicals used in this study were of analytical reagent (AR) standard.

Methods

For each adsorption test, a certain amount of quinoline stock solution of 1 g/L was pipetted to a 250 ml conical flask. Deionized water was added to the flask to make a quinoline solution. The concentration of this diluted solution in the flask was defined as the initial concentration. Coal powder was then added to the solution to adsorb quinoline. The conical flask was sealed with a plastic wrap and shaken in a thermostatic water bath shaker at a set temperature for a set time. After shaking, the solution was filtered using a Buchner funnel and vacuum pump. The filtrate was analyzed using a UV-vis spectrophotometer (UV-4802S, Shangkuo Instrument Technology Co., Ltd) to determine the residual concentration of quinoline in the solution. The maximum absorbance wavelength of quinoline was found to be 277 nm. To explore the effect of inorganic salt ions on the adsorption process, different amounts of NaCl or $CaCl_2$ were added to the quinoline solution before adsorption. Also, deionized water was used instead of simulated quinoline wastewater for a blank test, to eliminate the possibility that the dissolved organic matter on the surface of coal could interfere with the absorbance of the UV-vis spectrophotometer.

Equation (1) shows the calculation of the adsorption amount of the coal powder, Q_t, at the time t:

$$Q_t = \frac{(C_0 - C_t)V}{m} \tag{1}$$

The equilibrium adsorption amount, Q_e, was calculated by:

$$Q_e = \frac{(C_0 - C_e)V}{m} \tag{2}$$

The calculation of the removal rate of quinoline in the solution after time t is shown in Equation (3):

$$R_t = \frac{(C_0 - C_t)}{C_0} \times 100\% \qquad (3)$$

In Equations (1)–(3), Q_t is the adsorption amount of coal powder at time t (mg/g), C_0 is the initial concentration of the quinoline solution (mg/L), C_t is the concentration of quinoline in the solution at time t (mg/L), V is the volume of the quinoline solution (L), m is the dosage of coal powder (g), Q_e is the equilibrium adsorption amount (mg/g), C_e is the residual concentration of quinoline in solution at adsorption equilibrium (mg/L) and R_t is the removal rate of quinoline in the solution after the time t (%).

Coal powder adsorbent suspensions were prepared for ζ-potential measurement by ζ-potential analyzer (Model ZetaPALS, Brookhaven Instruments). Each suspension had a volume of 50 ml and the concentration of coal was 10 g/L. NaCl or $CaCl_2$ was added to make adsorbent suspensions containing different inorganic salt ions. Each suspension was stirred at 1,600 rpm for 5 min using a magnetic thermostatic mixer. After one night, 5 ml supernatant was transferred to the electrophoresis tank of the ζ-potential analyzer to measure the ζ-potential of the coal particle surfaces without adjusting the pH.

RESULTS AND DISCUSSION

Adsorbent coal properties

Through the XRF and XRD analysis shown in Table 1 and Figure 1, the content of inorganic components in the coal was relatively low. Quartz and morganite were the two main inorganic substances found in the coal sample. The lower content of clay minerals was good for the subsequent solid-liquid separation process (Zhang *et al.* 2003).

As shown in Figure 2, the coal surface was rough and uneven. This porous structure on the coal surface undoubtedly increased the possibility of pollutant adsorption. The mean pore size was found to be 8.176 nm, which was
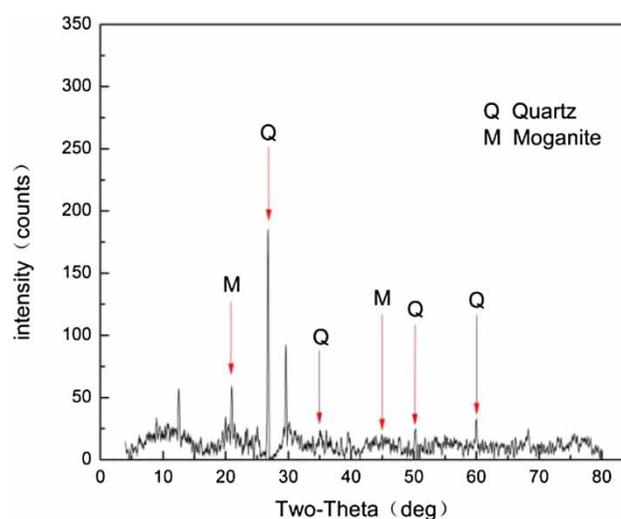

Figure 1 | X-ray diffraction patterns of the coal used in this study. (The X-ray tube voltage was 40 kV, the current was 30 mA, the anode target material Cu target, the radiation Ka.)

determined by a BET automatic nitrogen adsorption instrument. The specific surface area, total pore volume and mesopore volume of the pulverized coal were 13.131 m^2/g, 0.01253 cm^3/g and 0.012105 cm^3/g. The coal powder had a smaller specific surface area and total pore volume, but it had a more mesoporous structure, as shown in Figure 3, which is better for adsorbing large molecule pollutants from effluents.

Effect of inorganic salt ions

NaCl and $CaCl_2$ were added to the solution to investigate the effect of inorganic salt ions on the adsorption of quinoline using coal powder, with concentrations of Na^+ and Ca^{2+} from 0 to 100 mmol/L, $C_0 = 30$ mg/L, $m = 20$ g/L, $t = 60$ min, $T = 293$ K, without adjusting the pH, and the results are shown in Figure 4. When the concentration of Na^+ or Ca^{2+} increased from 0 to 8 mmol/L, the removal rate and adsorbed amount increased rapidly with an increase in the concentration of Na^+ or Ca^{2+}. The removal rate and adsorbed amount of quinoline reached 94.47%, 1.42 mg/g or 90.21%, 1.35 mg/g when the concentration of Ca^{2+} or Na^+ was 8 mmol/L, higher than the results obtained without the use of inorganic salts, which were 83.87%, 1.26 mg/g.

Interestingly, the removal rate and adsorption capacity showed a slow and steady increase when the concentration exceeded 8 mmol/L. This might be due to the fact that the addition of inorganic salts reduces the surface charge of the coal particles and compresses the electric double layer,
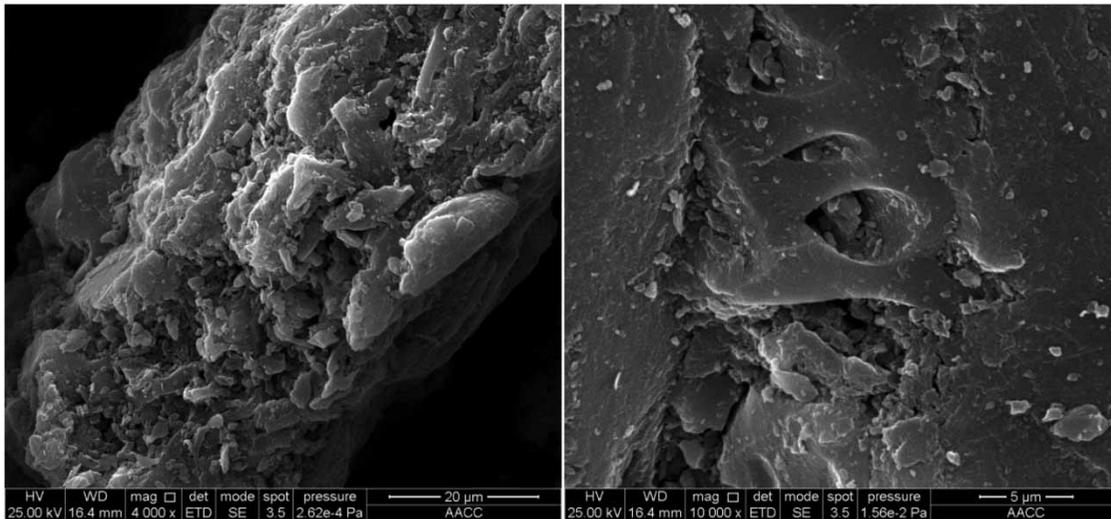
Table 1 | The results of XRF quantitative analysis of coal

Molecular formula	SiO_2	CaO	Al_2O_3	Fe_2O_3	MgO	K_2O	Na_2O
Content (%)	4.5	2.44	1.94	1.60	0.23	0.14	0.11

Figure 2 │ Surface morphologies of the coal powder used in this study. (The scanning acceleration voltage was 30 kV, the resolution was less than 3 nm, coating treatment was sprayed on before the test.)
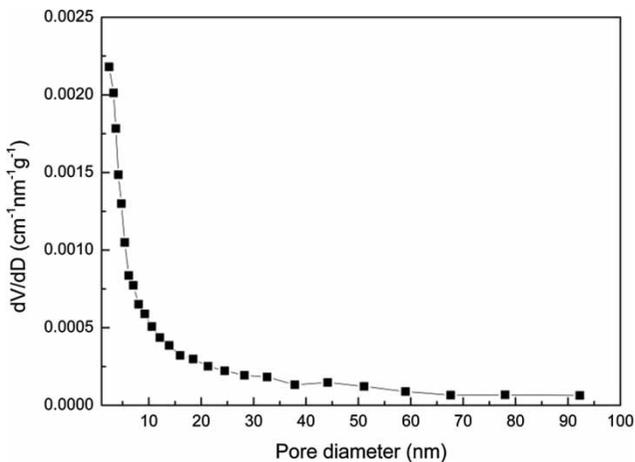

Figure 3 │ Pore size distribution of the coal powder used in this study.

Figure 4 │ Effect of Na^+ and Ca^{2+} on the removal and adsorption of quinoline by coal. ($C_0 = 30$ mg/L, $m = 20$ g/L, $t = 60$ min, $T = 293$ K).

thereby facilitating the motion of quinoline molecules onto the coal surface and enhancing adsorption (Bjelopavlic *et al.* 1999). In addition, the electric field around Na^+ and Ca^{2+} might cause a strong electrostatic effect between the inorganic salt ions and water molecules in the quinoline solution, making water molecules gather around ions and enhancing the binding force between water molecules in the quinoline solution; the reduction of free water relative to quinoline molecules favors the adsorption process (Arafat *et al.* 1999).

Figure 5 shows the changes in ζ-potential of the coal particle surface in different Na^+ and Ca^{2+} solutions. The
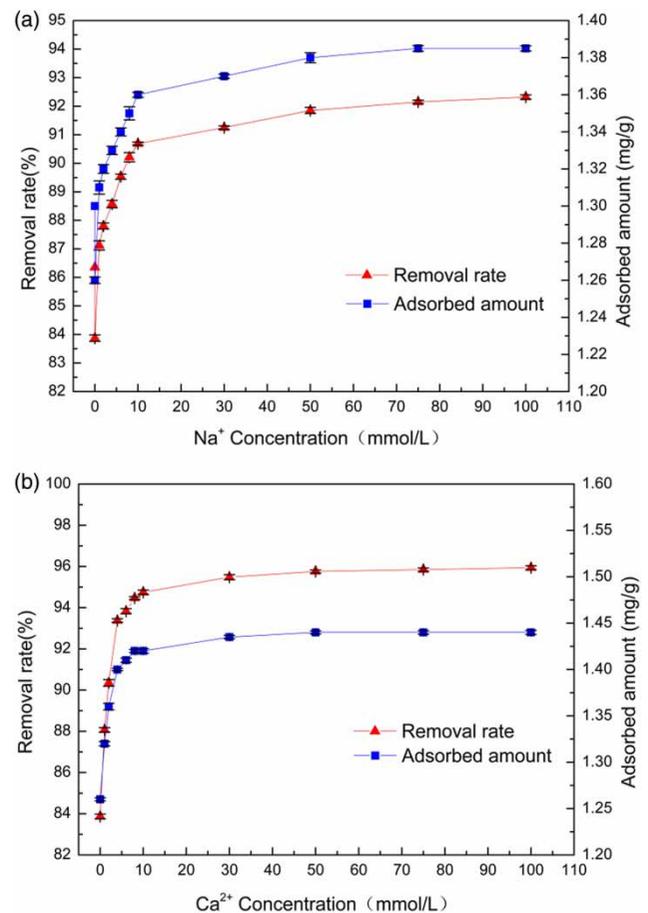
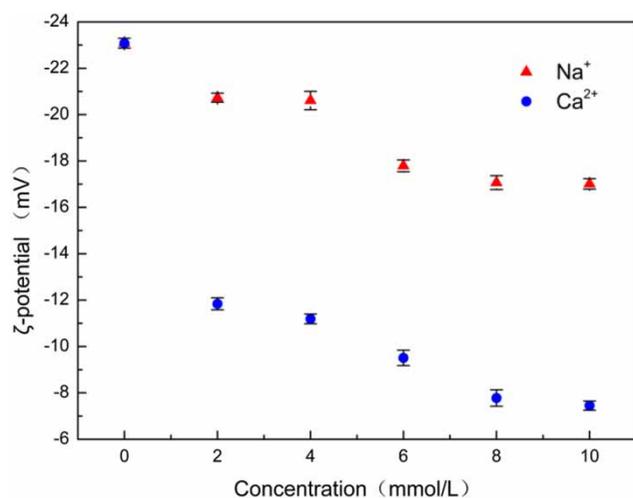**Figure 5** | ζ-potential of coal particles in the inorganic salt ion solution.

absolute value of ζ-potential tended to decrease gradually with the increase in the Na^+ or Ca^{2+} concentration. According to the Stern double layer model, the electrical double layer is divided into an adsorption layer and a diffusion layer. The inorganic salt ions compressed the diffusion layer, and reduced the repulsion potential energy. Na^+ and Ca^{2+} could exclude counter ions in the diffusion layer with the same symbol charge as the adsorption layer, thereby reducing the amount of charge on the surface of the coal particles, which was expressed the as ζ-potential absolute value decrease. In addition, Ca^{2+} brought more positive charge than Na^+ at the same concentration, causing a lower ζ-potential. The result indicated that Ca^{2+} had a beneficial effect on the adsorption of quinoline onto coal.

Adsorption isotherm modeling and calculation of thermodynamic parameters

The isothermal adsorption experiments were carried out with inorganic salt ions at three temperatures: 293 K, 303 K and 313 K. Each temperature was applied to the blank (without adding inorganic salt ions), adding Na^+ and Ca^{2+}, with concentration of Na^+ or Ca^{2+} 8 mmol/l, C_0 from 5 to 50 mg/L, $m = 20$ g/L, $t = 60$ min, and without adjusting the pH. The results are shown in Figure 6.

The results showed that the adsorption of quinoline by coal decreased with the increase of temperature, therefore the adsorption of quinoline by coal is an exothermic process. The adsorption isotherm described the relationship between the adsorbed amount of adsorbate molecules on the surface of the adsorbent and the
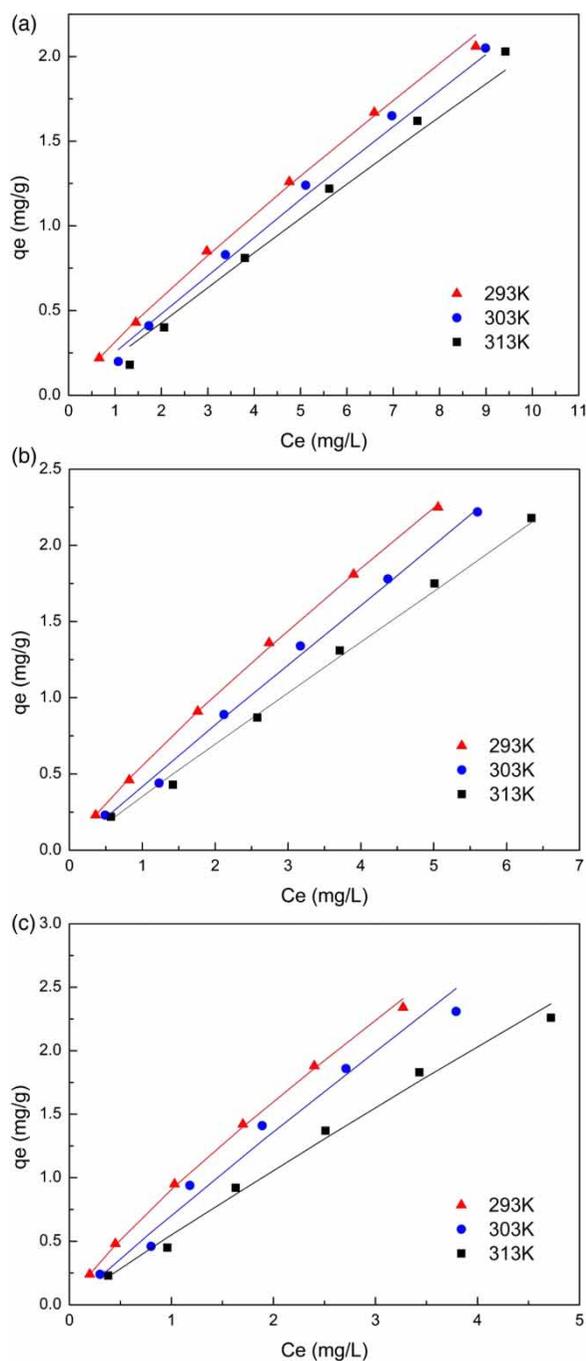

Figure 6 | Adsorption isotherms of the blank (a), Na^+ (b) and Ca^{2+} (c). (Experimental data points given by symbols and the lines predicted by the Freundlich isotherm model; concentration of Na^+ or Ca^{2+} 8 mmol/l, C_0 from 5 to 50 mg/L, $m = 20$ g/L, $t = 60$ min.)

concentration of the adsorbate molecules in the solution when the adsorption of the adsorbate molecules on the adsorbent surface reaches equilibrium under constant temperature conditions (Rameshraja & Srivastava 2012). Langmuir and Freundlich isotherms were used to fit the

Table 2 | Isothermal adsorption model fitting results

Langmuir isotherm

T/K	Condition	K_L (L/mg)	q_m (mg/g)	R^2
293	Blank	0.0614	5.5133	0.9986
	NaCl	0.1336	4.9517	0.9977
	CaCl$_2$	0.2784	4.4174	0.9989
303	Blank	0.0335	7.8401	0.9907
	NaCl	0.0608	7.5386	0.9855
	CaCl$_2$	0.1097	7.2036	0.9759
313	Blank	0.0304	7.7149	0.9909
	NaCl	0.0581	6.7146	0.9849
	CaCl$_2$	0.0967	6.4057	0.9850

Freundlich isotherm

T/K	Condition	K_F (L/mg)	1/n	R^2
293	Blank	0.3146	0.8806	0.9992
	NaCl	0.5556	0.8682	0.9998
	CaCl$_2$	0.9058	0.8244	0.9995
303	Blank	0.2487	0.9525	0.9929
	NaCl	0.4173	0.9744	0.9919
	CaCl$_2$	0.7040	0.9476	0.9789
313	Blank	0.2207	0.9655	0.9944
	NaCl	0.3510	0.9802	0.9918
	CaCl$_2$	0.5482	0.9438	0.9907

isotherm data, and the fitting results of constants and correlation coefficients in the adsorption models are shown in Table 2.

The Langmuir isothermal adsorption Equation (4) and linear expression (5) (Langmuir 1918) are as follows:

$$Q_e = \frac{K_L q_m C_e}{1 + K_L C_e} \tag{4}$$

$$\frac{C_e}{Q_e} = \frac{C_e}{q_m} + \frac{1}{K_L q_m} \tag{5}$$

where K_L is the Langmuir adsorption constants (L/mg), q_m is the monolayer adsorption capacity (mg/g).

The Freundlich isothermal adsorption Equation (6) and linear expression (7) (Freundlich 1906) are as follows:

$$Q_e = K_F C_e^{1/n} \tag{6}$$

$$\ln Q_e = \ln K_F + \frac{1}{n} \ln C_e \tag{7}$$

where K_F is the Freundlich adsorption constants (L/mg), $1/n$ is the parameter for evaluating the level of adsorption.

Comparing the values of the correlation coefficient R^2, the Freundlich isothermal adsorption model had a better correlation with the adsorption of quinoline by coal, and the isothermal adsorption curve was fitted as shown in Figure 6. The surface of the coal powder was dominated by aromatic rings, and the quinoline molecules could have coordination or complexation adsorption. The adsorption state was mainly physical adsorption. Also, as there was surface and pore adsorption, the Freundlich isothermal adsorption model was more suitable. The empirical parameter $1/n$ of the Freundlich isothermal adsorption model was less than 1, indicating that the adsorption of quinoline by coal is favorable. The value of K_F, which characterized the capacity for adsorption, was higher at the lowest temperature. Furthermore, the addition of NaCl and CaCl$_2$ produced a higher K_F than the blank, the K_F had the highest value with the addition of CaCl$_2$ at 293 K. This indicated that the inorganic salt ions could promote the adsorption of quinoline by coal powder. The addition of inorganic salt ions could reduce the electrostatic repulsion between coal particles and quinoline molecules, and the electric field around the salt ions caused the water molecules in the quinoline solution to accumulate around the ions, so the free water was reduced, resulting in the enhancement of adsorption and K_F value.

The Gibbs free energy ($\Delta G°$) of the system was used to describe the spontaneous extent of the adsorption. The $\Delta G°$ can be calculated as (Namasivayam & Kavitha 2002; Gupta et al. 2004; Günay et al. 2007):

$$\Delta G° = -RT \ln K \tag{8}$$

At a constant temperature, the Gibbs free energy is related to the heat of adsorption and the entropy change. It can be expressed as follows:

$$\Delta G° = \Delta H° - T\Delta S° \tag{9}$$

Equations (10) and (11) are obtained as:

$$\ln K = -\frac{\Delta H°}{RT} + \frac{\Delta S°}{R} \tag{10}$$

where $\Delta G°$ is the Gibbs free energy change (kJ/mol), $\Delta H°$ is the enthalpy change (kJ/mol), R is molar gas constant (R = 8.314 J/(mol*K)), T is temperature (K), $\Delta S°$ is the entropy change (J/mol·K), K is the distribution ratio.

The values of lnK at different temperatures could be obtained by plotting $ln(Q_{eq}/C_{eq})$ versus Q_{eq} and extending the line to the intercept. Afterwards, the values of $\Delta H°$ and

Table 3 | Values of thermodynamic parameters for the adsorption of quinoline by coal at different temperatures

T/K	lnK			$\Delta H°$ (kJ/mol)			$\Delta S°$ (J/mol·K)			$\Delta G°$ (kJ/mol)		
	Blank	NaCl	CaCl$_2$	Blank	NaCl	CaCl$_2$	Blank	NaCl	CaCl$_2$	Blank	NaCl	CaCl$_2$
293	3.75	4.39	5.03							−9.07	−10.65	−12.26
303	3.31	3.89	4.58	−26.71	−31.84	−33.99	−60.18	−72.33	−74.15	−8.47	−9.92	−11.53
313	3.05	3.56	4.14							−7.87	−9.19	−10.78

$\Delta S°$ were calculated from the slope and intercept of plots of *lnK* versus *1/T*. Further, $\Delta G°$ was obtained using Equation (9). The values of the thermodynamic parameters are shown in Table 3.

The negative value of $\Delta G°$ showed that the adsorption of quinoline by coal was spontaneous, and the absolute values of $\Delta G°$ under the addition of inorganic salt ions were higher than that of the blank condition, which indicated that the inorganic salt ions intensified the adsorption of quinoline. The negative value of $\Delta H°$ showed clearly that the adsorption of quinoline by coal was exothermic, and the lower temperature favored the adsorption. The degree of freedom of quinoline molecules on the coal powder surface reduced after adsorption, indicated by the negative value of $\Delta S°$.

Kinetics of adsorption and calculation of adsorption activation energy

Figure 7 shows the effect of adsorption time on the adsorption of quinoline by coal in the presence of inorganic salt ions, at temperatures of 293 K, 303 K and 313 K. For this test, the adsorption time was 10 to 120 min, with concentrations of 8 mmol/L Na$^+$ or Ca^{2+}, $C_0 = 30$ mg/L, $m = 20$ g/L, and without adjusting the pH.

The amount of quinoline adsorbed increased with adsorption time in the blank, Na$^+$ and Ca^{2+}, and increased rapidly in the first 30 min, and then plateaued after 60 min. In addition, it could be seen that the adsorption capacity was larger under the lower temperature with the same adsorption time.

The pseudo-first-order model and pseudo-second-order model were used to study the adsorption kinetics of quinoline, and the fitting results are shown in Table 4.

The pseudo-first-order model is as follows (Ho & McKay 1999):

$$\frac{dQ_t}{dt} = k_1(Q_e - Q_t) \tag{11}$$

Integral expression:

$$Q_t = Q_e(1 - e^{-k_1 t}) \tag{12}$$

Linear expression:

$$\log(Q_e - Q_t) = logQ_e\left(-\frac{k_1}{2.303}\right)t \tag{13}$$

Boundary conditions:

$$t = 0, \quad Q_t = 0; \quad t = t, \quad Q_t = Q_e \tag{14}$$

where k_1 is the rate constant of pseudo-first-order adsorption (min^{-1}).

The pseudo-second-order model is as follows (Ho & McKay 1998):

$$\frac{dQ_t}{dt} = k_2(Q_e - Q_t)^2 \tag{15}$$

Integral expression:

$$\frac{1}{(Q_e - Q_t)} = \frac{1}{Q_e} + k_2 t \tag{16}$$

Linear expression:

$$\frac{t}{Q_t} = \frac{1}{k_2 Q_e^2} + \frac{t}{Q_e} \tag{17}$$

Boundary conditions:

$$t = 0, \quad Q_t = 0; \quad t = t, \quad Q_t = Q_e \tag{18}$$

At $t \to 0$, the initial adsorption rate h (mg/(g·min)) is as follows:
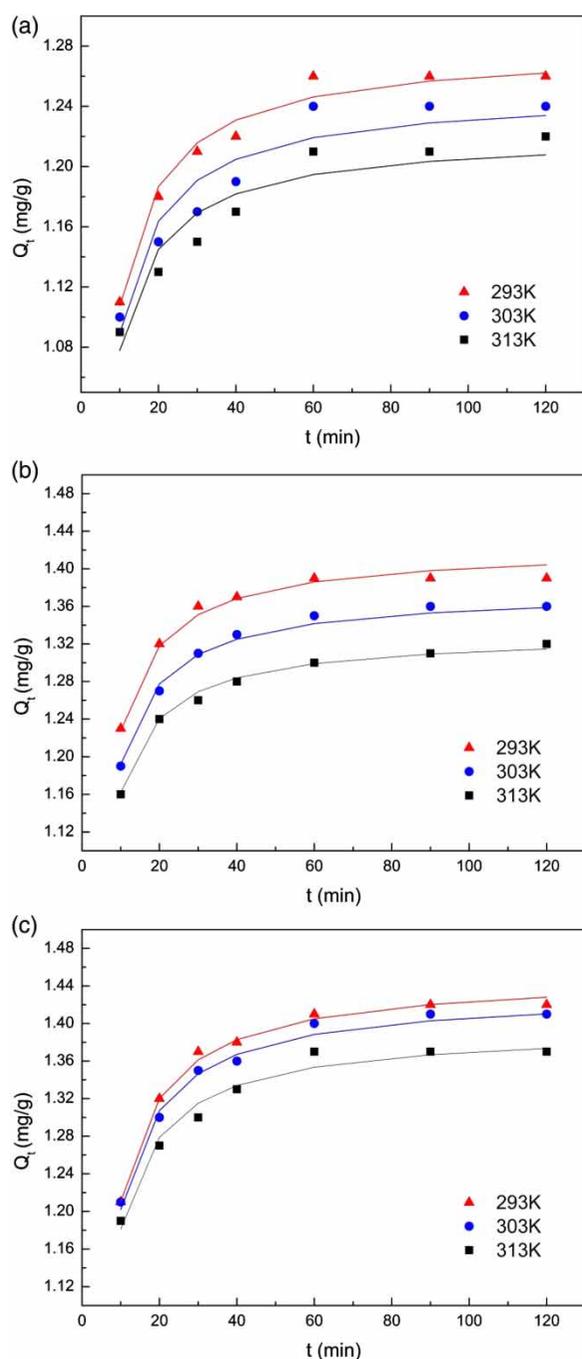
$$h = k_2 \times Q_e^2 \tag{19}$$

Figure 7 | Effect of adsorption time on adsorption in the blank (a), Na⁺ (b) and Ca²⁺ (c) conditions. (Experimental data points given by symbols and the lines predicted by the pseudo-second-order model; concentration of 8 mmol/L Na⁺ or Ca²⁺, $C_0 = 30$ mg/L, $m = 20$ g/L.)

where k_2 is the rate constant of pseudo-second-order adsorption (g/(mg·min)).

The pseudo-first-order model had a lower correlation coefficient R^2, and the calculated equilibrium adsorption amount $Q_{e(cal)}$ was much lower than the actual equilibrium adsorption $Q_{e(exp)}$, indicating that pseudo-first-order cannot fit the adsorption of quinoline. The pseudo-second-order model has a good value of R^2, and the equilibrium adsorption amount was close to the actual equilibrium adsorption amount. So the pseudo-second-order model can be used to describe the adsorption process of quinoline by coal; the curve is shown in Figure 7.

The adsorption rate of quinoline decreased gradually in the blank, Na⁺ and Ca²⁺ conditions, shown by the changing trend of k_2, which was the rate constant of pseudo-second-order model. This was due to the electric field around the inorganic salt ions causing the water molecules in the solution to collect around the ions, leading to a decrease in free water and a reduction in quinoline solubility. The probability of collision between the quinoline molecules increased, resulting in increased diffusion resistance.

As can be seen from Table 4, the adsorption of quinoline by coal under different temperatures and conditions accords with the pseudo-second-order model, so the activation energy can be calculated by the Arrhenius formula (Chandra *et al.* 2007):

$$k_2 = k_0 \exp\left(-\frac{E_a}{RT}\right) \tag{20}$$

Equation (20) is logarithmic on both sides:

$$\ln k_2 = \ln k_0 - \frac{E_a}{RT} \tag{21}$$

where k_2 is the rate constant of pseudo-second-order adsorption (g/(mg·min)), k_0 is preexponential factor, and E_a is activation energy (KJ·mol⁻¹).

The activation energy could be obtained by the slope of the plot of lnk_2 versus $10^3/T$ as shown in Figure 8. The activation energies of the adsorption reaction were 7.38 kJ/mol, 6.08 kJ/mol and 5.31 kJ/mol respectively in the blank, Na⁺ and Ca²⁺ conditions. The activation energy required for physical adsorption is very small, usually in the range of 5–40 kJ/mol. But for chemical adsorption, it is generally greater than 83.72 kJ/mol (Sun *et al.* 2014). The result indicated that the adsorption of quinoline by coal was physical adsorption, and a small activation energy corresponds to a easy adsorption process. The values of activation energy with Na⁺ and Ca²⁺ were smaller than that of the blank, which suggested that inorganic salt ions were favorable to the adsorption of quinoline by coal powder.

Table 4 | Kinetic model fitting results

Pseudo-first-order

T/K	Condition	$Q_{e(exp)}$ (mg/g)	$Q_{e(cal)}$ (mg/g)	k_1 (min^{-1})	R^2
293	Blank	1.28	0.14	0.0213	0.8701
	NaCl	1.39	0.12	0.0298	0.8564
	CaCl$_2$	1.42	0.16	0.0258	0.8582
303	Blank	1.24	0.16	0.0288	0.8786
	NaCl	1.36	0.14	0.0221	0.8565
	CaCl$_2$	1.41	0.19	0.0279	0.8939
313	Blank	1.24	0.15	0.0179	0.8862
	NaCl	1.32	0.14	0.0216	0.9221
	CaCl$_2$	1.37	0.19	0.0336	0.9260

Pseudo-second-order

T/K	Condition	$Q_{e(cal)}$ (mg/g)	k_2 (g/(mg·min))	h (mg/(g·min))	R^2
293	Blank	1.29	0.5069	0.829	0.9823
	NaCl	1.42	0.4427	0.896	0.9887
	CaCl$_2$	1.45	0.3459	0.729	0.9954
303	Blank	1.25	0.5467	0.853	0.9195
	NaCl	1.38	0.4702	0.891	0.9961
	CaCl$_2$	1.43	0.3634	0.746	0.9882
313	Blank	1.22	0.6155	0.918	0.9145
	NaCl	1.33	0.5195	0.919	0.9960
	CaCl$_2$	1.39	0.3978	0.773	0.9807
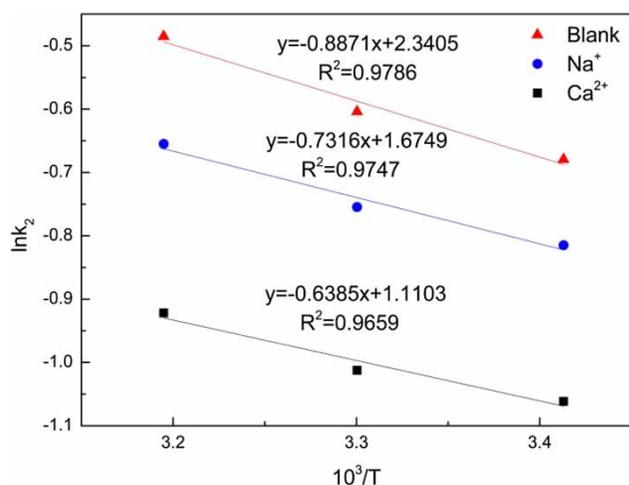
Figure 8 | Calculation of activation energy in the blank, Na$^+$ and Ca^{2+}.

CONCLUSIONS

It was feasible to adsorb quinoline using coal powders as the adsorbent, as indicated by the experimental results. The addition of an appropriate amount of inorganic salt ions (Na$^+$ or Ca^{2+}) to the solution significantly improved the adsorption effect, as an increase in both the removal rate and adsorption capacity of quinoline was found. $\Delta G°$ was negative, indicating that the adsorption of quinoline by coal was spontaneous. The higher absolute value of $\Delta G°$ and the smaller activation energy E_a of the adsorption reaction identified when Na$^+$ or Ca^{2+} was added suggest that the inorganic salt ions could enhance the adsorption of quinoline. Negative $\Delta H°$ suggested the adsorption was an exothermic process and negative $\Delta S°$ indicated more quinoline molecules adsorbed on the surface of the coal powder.

The addition of inorganic salt ions could reduce the ζ-potential of coal particles and the electrostatic repulsion between coal particles and quinoline molecules, which was beneficial for quinoline molecules moving to the surface of coal powder to enhance adsorption. In addition, the electric field around Na$^+$ or Ca^{2+} could make a strong electrostatic interaction with the water molecules in the quinoline solution. The water molecules gathered around the ions and enhanced the binding force between water molecules in quinoline solution. The free water for the quinoline molecules decreased accordingly, which was also beneficial for the adsorption process.

REFERENCES

Arafat, H. A., Marcus, F. A. & Pinto, N. G. 1999 Effect of salt on the mechanism of adsorption of aromatics on activated carbon. *Langmuir* **15**, 5997–6003.

Bjelopavlic, M., Newcombe, G. & Hayes, R. 1999 Adsorption of NOM onto activated carbon: effect of surface charge, ionic strength, and pore volume distribution. *Journal of Colloid & Interface Science* **210**, 271–280.

Chandra, T. C., Mirna, M. M., Sudaryanto, Y. & Ismadji, S. 2007 Adsorption of basic dye onto activated carbon prepared from durian shell: studies of adsorption equilibrium and kinetics. *Chemical Engineering Journal* **127**, 121–129.

Chen, J. 2002 Adsorption of quinoline to kaolinite and montmorillonite. *Environmental Engineering Science* **19**, 59–68.

Freundlich, H. M. F. 1906 Over the adsorption in solution. *J. Phys. Chem.* **57**, 385–471.

Gao, L., Li, S., Wang, Y. & Sun, H. 2015 Organic pollution removal from coke plant wastewater using coking coal. *Water Science & Technology A Journal of the International Association on Water Pollution Research* **72**, 158–163.

Gao, L., Li, S. & Wang, Y. 2016a Effect of different pH coking wastewater on adsorption of coking coal. *Water Science & Technology A Journal of the International Association on Water Pollution Research* **73**, 582–587.

Gao, L., Li, S., Wang, Y., Gui, X. & Xu, H. 2016b Pretreatment of coking wastewater by an adsorption process using fine coking coal. *Physicochemical Problems of Mineral Processing* **52**, 422–436.

Günay, A., Arslankaya, E. & Tosun, I. 2007 Lead removal from aqueous solution by natural and pretreated clinoptilolite: adsorption equilibrium and kinetics. *Journal of Hazardous Materials* **146**, 362–371.

Gupta, V. K., Singh, P. & Rahman, N. 2004 Adsorption behavior of Hg(II), Pb(II), and Cd(II) from aqueous solution on Duolite C-433: a synthetic resin. *Journal of Colloid & Interface Science* **275**, 398–402.

Hao, S., Wen, J., Yu, X. & Chu, W. 2013 Effect of the surface oxygen groups on methane adsorption on coals. *Applied Surface Science* **264**, 433–442.

Ho, Y. S. & McKay, G. 1998 Sorption of dye from aqueous solution by peat. *Chemical Engineering Journal* **70**, 115–124.

Ho, Y. S. & McKay, G. 1999 The sorption of lead (II) ions on peat. *Water Research* **33**, 578–585.

Jian, K., Fu, X., Ding, Y., Wang, H. & Li, T. 2015 Characteristics of pores and methane adsorption of low-rank coal in China. *Journal of Natural Gas Science & Engineering* **27**, 207–218.

Langmuir, I. 1918 The adsorption of gases on plane surfaces of glass, mica and platinum. *J. Am. Chem. Soc.* **40**, 1361–1403.

Namasivayam, C. & Kavitha, D. 2002 Removal of Congo Red from water by adsorption onto activated carbon prepared from coir pith, an agricultural solid waste. *Dyes & Pigments* **54**, 47–58.

Padoley, K. V., Mudliar, S. N. & Pandey, R. A. 2008 Heterocyclic nitrogenous pollutants in the environment and their treatment options--an overview. *Bioresource Technology* **99**, 4029–4043.

Rameshraja, D. & Srivastava, V. C. 2012 Quinoline adsorption onto granular activated carbon and bagasse fly ash. *Chemical Engineering Journal* **181–182**, 343–351.

Santarossa, G., Iannuzzi, M., Vargas, A. & Baiker, A. 2008 Adsorption of naphthalene and quinoline on Pt, Pd and Rh: a DFT study. *Chemphyschem* **9**, 401–413.

Sun, Y., Yue, Q., Mao, Y., Gao, B., Gao, Y. & Huang, L. 2014 Enhanced adsorption of chromium onto activated carbon by microwave-assisted H 3 PO 4, mixed with Fe/Al/Mn activation. *Journal of Hazardous Materials* **265**, 191–200.

Thomas, J. K., Gunda, K., Rehbein, P. & Ng, F. T. T. 2010 Flow calorimetry and adsorption study of dibenzothiophene, quinoline and naphthalene over modified Y zeolites. *Applied Catalysis B Environmental* **94**, 225–233.

Vico, L. I. & Acebal, S. G. 2006 Some aspects about the adsorption of quinoline on fibrous silicates and Patagonian saponite. *Applied Clay Science* **33**, 142–148.

Wang, Y., Liu, L., Zhang, M., Tong, J., Zhou, J., Zhang, H. & Gao, L. 2014 A process of coking wastewater treatment. Chinese patent 10101496.7.4, 595–601.

Wang, C., Ma, K., Wu, T., Ye, M., Tan, P. & Yan, K. 2016 Electrochemical mineralization pathway of quinoline by boron-doped diamond anodes. *Chemosphere* **149**, 219–223.

Zhang, M., Wang, Y. & Liu, J. 2003 Utilization of mineral processing flocculants in dewatering of coal slimes. *China Coal* **29**, 46–47.

Zhu, S., Bell, P. R. F. & Greenfield, P. F. 1995 Quinoline adsorption onto combusted Rundle spent shale in dilute aqueous solution at the natural pH 8. *Water Research* **29**, 1393–1400.